

Spectral analysis of ^{99m}Tc -HMPAO for estimating cerebral blood flow: a comparison with H_2^{15}O PET

Masashi TAKASAWA,* Kenya MURASE,** Naohiko OKU,* Minoru KAWAMATA,** Makoto NAGAYOSHI,**
Masao IMAIZUMI,* Takuya YOSHIKAWA,**** Yasuhiro OSAKI,* Yasuyuki KIMURA,*
Katsufumi KAJIMOTO,* Kazuo KITAGAWA,**** Masatsugu HORI*** and Jun HATAZAWA*

*Department of Nuclear Medicine and Tracer Kinetics, Osaka University Graduate School of Medicine

**Department of Allied Health Sciences, Osaka University Graduate School of Medicine

***Division of Strokeology, Department of Internal Medicine and Therapeutics, Osaka University Graduate School of Medicine

Cerebral blood flow (CBF) can be quantified non-invasively using the brain perfusion index (BPI), which is determined using radionuclide angiographic data obtained through the use of technetium-99m hexamethylpropylene amine oxime (^{99m}Tc -HMPAO). The BPI is generally calculated using graphical analysis (GA). In this study, BPI was measured using spectral analysis (SA), and the usefulness of SA was compared with that of GA. Thirteen patients with various brain diseases and four healthy male volunteers were examined using radionuclide angiography with ^{99m}Tc -HMPAO. The BPI was measured for each subject using both SA and GA. In the four healthy volunteers, the BPI was examined at rest and after the intravenous administration of 1 g of acetazolamide (ACZ). An H_2^{15}O PET examination was also performed in the 13 patients; the BPI^{S} and BPI^{G} values were compared with the CBF measurements obtained using H_2^{15}O PET (CBF^{PET}). The BPI values obtained by SA (BPI^{S}) (x) and by GA (BPI^{G}) (y) were correlated ($y = 0.568x + 0.055$, $r = 0.901$) in the 13 patients and four healthy volunteers at rest, although the BPI^{G} values were underestimated by $36.1 \pm 7.5\%$ (mean \pm SD) compared with the BPI^{S} values. The degree of underestimation tended to increase with increasing BPI^{S} values. The increase in the BPI^{S} was $32.1 \pm 8.0\%$ after the intravenous administration of ACZ, while the increase in BPI^{G} was only $8.1 \pm 2.8\%$. This discrepancy was considered to be the result of the BPI^{G} values being affected by the first-pass extraction fraction of the tracer. Although both BPI^{S} and BPI^{G} values were significantly correlated with the CBF^{PET} values, the correlation coefficient for BPI^{S} was higher than that for BPI^{G} (BPI^{S} : $r = 0.881$; BPI^{G} : $r = 0.832$). These results suggest that SA produces a more reliable BPI for quantifying CBF using ^{99m}Tc -HMPAO than the conventional method using GA. The SA method should be especially useful for activation studies involving pharmacological intervention and/or clinical cases with an increased CBF.

Key words: brain perfusion index, cerebral blood flow, spectral analysis, graphical analysis, single-photon emission tomography

INTRODUCTION

SEVERAL REVIEWS INDICATE that the quantitation of cerebral blood flow (CBF) is very important for patient management, especially in cases of cerebrovascular disease.¹ In particular, measuring the residual flow in the brain tissue can have a crucial impact on prognosis and therapeutic planning.^{2,3}

Matsuda et al. developed a simple non-invasive method of quantifying brain perfusion using technetium-99m

Received October 6, 2003, revision accepted February 9, 2004.

For reprint contact: Masashi Takasawa, M.D., Department of Nuclear Medicine and Tracer Kinetics, Osaka University Graduate School of Medicine, 2-2, Yamadaoka, Suita, Osaka 565-0871, JAPAN.

E-mail: tkswm@medone.med.osaka-u.ac.jp

Table 1 Clinical characteristics of the subjects

No./age/gender	Clinical Diagnosis	Location of Lesion on MRI	Lesion Size
1/73/M	Infarct	Lt. F, P, Rt. P	Large
2/75/M	Infarct	Rt. P	Large
3/67/M	Infarct	Lt. BG	Large
4/54/M	Infarct	Rt. O	Large
5/72/M	Infarct	Lt. P	Large
6/69/F	Infarct	Rt. BG	Large
7/74/M	Infarct	Rt. BG	Small
8/62/M	TIA	Rt. BG	Small
9/58/M	TIA	Rt. P, BG	Small
10/56/F	TIA	-	-
11/56/F	Silent Infarct	Bil. BG	Small
12/70/F	Hypertensive Encephalopathy	Bil. BG	Small
13/35/M	Seizure, Interictal	-	-

TIA, transient ischemic attack; Rt., right; Lt., left; Bil., bilateral; F, frontal lobe; P, parietal lobe; O, occipital lobe; BG, basal ganglia; Large, > 3cm; Small, ≤ 3cm in the long axis.

hexamethylpropylene amine oxime (^{99m}Tc -HMPAO)⁴ or technetium-99m ethyl cysteinate dimer (^{99m}Tc -ECD).⁵ They calculated the brain perfusion index (BPI) using graphical analysis (GA) of radionuclide angiographic data^{4,5} and obtained a regression equation between BPI and CBF as measured by xenon-133 inhalation and single-photon emission CT (SPECT).⁴ Regional CBF maps were then acquired using the calculated BPI and Lassen's linearization correction algorithm.⁶ However, the BPI obtained by means of GA (BPI^G) is derived from the unidirectional influx rate of the tracer to the brain, which is proportional to the product of the first-pass extraction fraction of the tracer and CBF. Therefore, this index does not accurately reflect CBF, because it is affected by the first-pass extraction fraction of the tracer, which generally changes, depending upon the CBF. Thus, a BPI measurement that reflects CBF more accurately and is not affected by the first-pass extraction fraction is required.

Spectral analysis (SA) was introduced by Cunningham and Jones to analyze dynamic positron emission tomography (PET) data.⁷ This method provides a spectrum of the kinetic components involved in the regional uptake and partitioning of a tracer from blood to tissues and allows the tissue impulse response function to be derived with minimal modeling assumptions.⁷

Murase et al. applied this SA method to dynamic SPECT data using ^{123}I -IMP,⁸ ^{99m}Tc -HMPAO and ^{99m}Tc -ECD⁹ to demonstrate its usefulness. However, there have not been any reports so far comparing BPI with absolute CBF measured by H_2^{15}O PET or studying the change in BPI after the intravenous administration of acetazolamide (ACZ).

In this study, we measured the BPI using SA (BPI^S) and ^{99m}Tc -HMPAO and investigated the degree of increase

both in BPI^S and BPI^G after the intravenous administration of ACZ. We also performed H_2^{15}O PET, which is the most reliable imaging modality currently available in clinical practice and, compared both BPI^S and BPI^G with absolute CBF.

PATIENTS, MATERIALS AND METHODS

Patients

Thirteen patients [nine males, four females; age, 63.5 ± 11.3 (mean \pm SD) years old] with various brain diseases (Table 1) and four healthy male volunteers (22 or 23 years old) participated in this study. Seven patients had chronic cerebral infarctions, three patients had experienced transient ischemic attacks (TIA) and were in a chronic stage, one patient suffered from a silent infarction, one patient had hypertensive encephalopathy, and one patient had a seizure. Informed consent was obtained from each participant and their families after a detailed explanation of the purpose of the study and the scanning procedures.

Measurement of BPI using ^{99m}Tc -HMPAO

For the radionuclide angiography, a bolus of 370–740 MBq ^{99m}Tc -HMPAO was injected intravenously (a few seconds), followed by sequential imaging in the supine position with the front of the body placed against a gamma camera equipped with low-energy high-resolution collimator (RC-2600i, Hitachi Medical Co., Tokyo, Japan) to bring both the brain and the heart into the field of view. The passage of the tracer from the aortic arch to the brain was monitored in a 128×128 matrix, each 1 sec in duration, over a total period of 100 sec.⁴

The four healthy volunteers underwent two radionuclide angiography examinations: once at rest and once ten

minutes after the injection of 1 g of ACZ. The two examinations were performed within a week of each other. We measured the BPI at rest [BPI_{rest}] and after ACZ administration [BPI_{ACZ}] in the four healthy volunteers. The rate of BPI increase (% change in BPI) was defined as follows:

$$\% \text{ change in BPI} = 100 \cdot \frac{[BPI_{ACZ}] - [BPI_{rest}]}{[BPI_{rest}]}$$

To calculate the BPI^S , the raw data were transferred to a Silicon Graphics workstation (Indigo 2; Silicon Graphics, Mountain View, CA, USA). Regions of interest (ROIs) were hand-drawn over the left and right brain hemispheres and the aortic arch using a Silicon Graphics workstation and a software package (Dr. View; Asahi Kasei Joho System Co., Ltd., Tokyo, Japan) without the use of a filter, as described by Matsuda et al.³ The time-activity curves in the brain and in the aortic arch were manually fitted. The BPI^S calculations were performed on a Silicon Graphics workstation using a software package for BPI analysis that was developed by Murase.⁹⁻¹¹

Using SA to calculate the ^{99m}Tc -HMPAO level, the level of radioactivity of ^{99m}Tc -HMPAO in the brain at a given time t [$C^s(t)$] was modeled as a convolution of the blood input function [$C_a(t)$] with a sum of k exponential terms, as shown by the following equation⁹:

$$C^s(t) = \sum_{i=0}^k \alpha_i \cdot \int_0^t C_a(u) e^{-\beta_i(t-u)} du \quad (\text{Eq. 1})$$

where α_i and β_i were assumed to be positive or zero. The upper limit, k , represents the maximum number of terms to be included in the model and was set at 1000. The α_i values were determined from Eq. 1 using the level of brain radioactivity measured by radionuclide angiography and the non-negative least-squares method for β_i ranging from 0 to 2 min^{-1} with an increment of 0.002 min^{-1} . In the present study, the amount of radioactivity in the aortic arch was taken as $C_a(t)$ in Eq. 1 to maximize the non-invasiveness of the procedure without the need for blood sampling. When $C_a(t)$ was replaced by Dirac's delta function in Eq. 1, the tissue impulse response function [$IRF^S(t)$] was given by the following equation:

$$IRF^S(t) = \sum_{i=0}^k \alpha_i \cdot e^{-\beta_i t} \quad (\text{Eq. 2})$$

The BPI (BPI^S) was calculated from $IRF^S(0)$ as follows:

$$BPI^S = \sum_{i=0}^k \alpha_i \quad (\text{Eq. 3})$$

where BPI^S has a unit of min^{-1} .

For the measurement of BPI^G , the raw data were transferred to a Hitachi workstation (RW-3000; Hitachi Medical Co., Tokyo, Japan). The BPI^G calculations were performed on a Hitachi workstation using a software package for Patlak plot analysis (RW-3000; Hitachi Medical Co., Tokyo, Japan) with no filter, as described previously by Matsuda et al.⁴

The BPI^G was calculated as follows:

$$BPI^G = 100 \cdot k_u \cdot \frac{10 \cdot ROI_{aorta}}{ROI_{brain}} \quad (\text{Eq. 4})$$

where ROI_{aorta} and ROI_{brain} represent the size of the aortic arch and brain hemisphere ROIs, respectively, and where k_u is the unidirectional influx rate of the tracer from the blood to the brain and is determined by the slope of the line in GA.⁴ To compare BPI^G with BPI^S , we multiplied the result of Eq. 4 by 0.06 so that the BPI^G and the BPI^S would have the same unit (min^{-1}).

The degree of the underestimation in BPI^G compared with BPI^S was calculated as follows:

$$\begin{aligned} \text{Underestimation rate} \\ = 100 \cdot \frac{[BPI^S] - [BPI^G]}{[BPI^S]} (\%) \end{aligned} \quad (\text{Eq. 5})$$

Measurement of absolute CBF using $H_2^{15}O$ PET

BPI and CBF, as measured using $H_2^{15}O$ PET (CBF^{PET}), were compared among 13 patients. Both ^{99m}Tc -HMPAO SPECT and $H_2^{15}O$ PET were performed within one week on the same patient.

PET was performed using a Headtome V scanner (Shimadzu Corp., Kyoto, Japan), which had a spatial resolution of 4.0 mm at full width at half maximum (FWHM). The subjects were placed in a supine position on a bed in a semi-dark room and asked to close their eyes. For attenuation correction, a transmission scan with a germanium-68/gallium-68 line source was obtained for each patient. The 13 patients received a 36-sec intravenous bolus of 1110 MBq $H_2^{15}O$ at a flow rate of 30 ml/min through a cannula placed in an antecubital vein.

Data were acquired over a scanning period of 160 sec using a 128×128 matrix. The regional cerebral blood flow was measured using the $H_2^{15}O$ bolus injection (autoradiographic) method while the patient was in a resting state.¹² To evaluate an input function, continuous arterial blood sampling from a catheter needle inserted in the radial artery was performed for 5 minutes at a speed of 5 ml/min and, concurrently measured the ^{15}O radioactivity with a beta-detector (Shimadzu Corp., Kyoto, Japan). The transaxial images were reconstructed using the ordered subsets expectation maximization (OSEM) method¹³; the final slice thickness was 3.1 mm.

The PET data were also transferred to a Silicon Graphics workstation. ROIs were drawn over the left and right whole brain hemispheres of the transaxial image on the workstation using the "Dr. View" software package. CBF^{PET} (ml/100 g/min) was calculated as the mean CBF of five slices ranging from the basal ganglia level to the upper parietal lobe level.

Statistical analysis

The correlations between BPI^S and BPI^G values and between the BPI and CBF^{PET} were assessed by linear

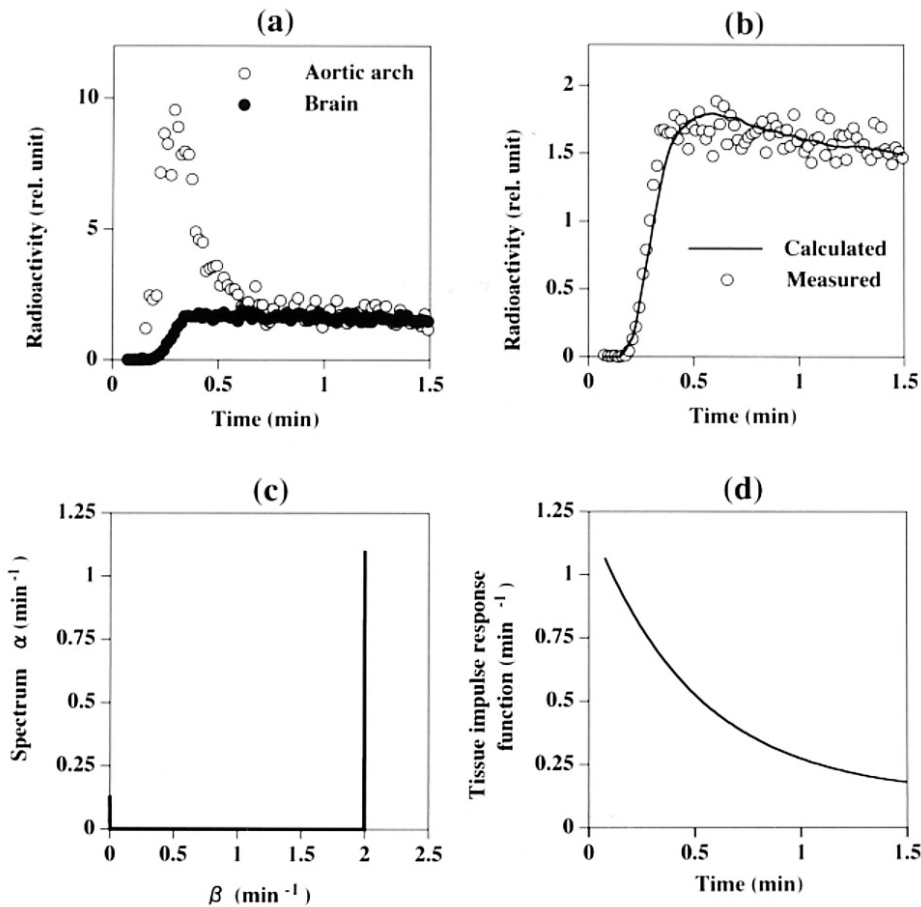


Fig. 1 Example of spectral analysis applied to radionuclide angiographic data obtained using ^{99m}Tc -HMPAO. a: Time-activity curves for ROIs in the aortic arch (*open circles*) and brain hemisphere (*closed circles*). b: Time-activity data, as calculated from Eq. 1, are shown by the solid line together with data measured in the brain hemisphere ROI (*open circles*). c: Spectral data of the tissue response. d: Corresponding tissue impulse response function calculated from Eq. 2.⁹

regression analysis. The comparison of the degree of increase in BPI^{S} and BPI^{G} values after ACZ injection was assessed using the Wilcoxon signed rank test. A p value of less than 0.05 was considered to be significant.

RESULTS

Figure 1 shows an example of SA applied to radionuclide angiographic data obtained using ^{99m}Tc -HMPAO. The time-activity curves for the aortic arch and the targeted brain hemisphere ROIs are shown (Fig. 1a). The spectral data for the tissue response (Fig. 1c) and the corresponding tissue impulse response function calculated from Eq. 2 (Fig. 1d) are also shown. The time-activity data calculated using Eq. 1 (*solid line*) and those measured in the brain hemisphere ROIs (*open circles*) are shown in Figure 1b.⁹

Figure 2 shows the relationship between the BPI^{S} and BPI^{G} values obtained from radionuclide angiographic data using ^{99m}Tc -HMPAO for all 13 patients and the four

healthy male volunteers at rest. The correlation between these data was statistically significant ($r = 0.901$), with a regression equation of $y = 0.568x + 0.055$. The BPI^{G} values were underestimated by $36.1 \pm 7.5\%$ (mean \pm SD) compared with the BPI^{S} values. The degree of underestimation tended to increase as the BPI^{S} values increased (Fig. 3).

We also studied the degree of increase in BPI after the intravenous administration of 1 g of ACZ in the four volunteers. The BPI^{S} was 1.054 ± 0.081 (mean \pm SD) at rest and 1.389 ± 0.077 after the venous administration of ACZ, respectively. The BPI^{G} was 0.696 ± 0.037 at rest and 0.752 ± 0.040 after ACZ administration, respectively. As shown in Figure 4, the percent change in BPI^{G} ($8.1 \pm 2.8\%$) was significantly lower than that in BPI^{S} ($32.1 \pm 8.0\%$).

The BPI and CBF^{PET} values are compared in Figure 5, which shows the relationship between the BPI^{S} (*open circles*) and the BPI^{G} values (*closed circles*) obtained using ^{99m}Tc -HMPAO and the CBF^{PET} values. The BPI^{S}

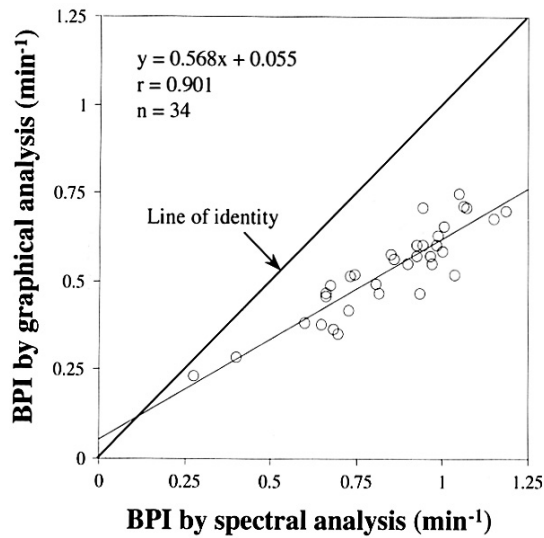


Fig. 2 Relationship between the brain perfusion index (BPI) values obtained by spectral analysis (SA) (x) and by graphical analysis (GA) (y) of radionuclide angiographic data generated by ^{99m}Tc -HMPAO. The correlation was statistically significant ($p < 0.01$). The BPI values obtained by GA were underestimated by $36.7 \pm 8.1\%$ (mean \pm SD) compared with those obtained by SA.

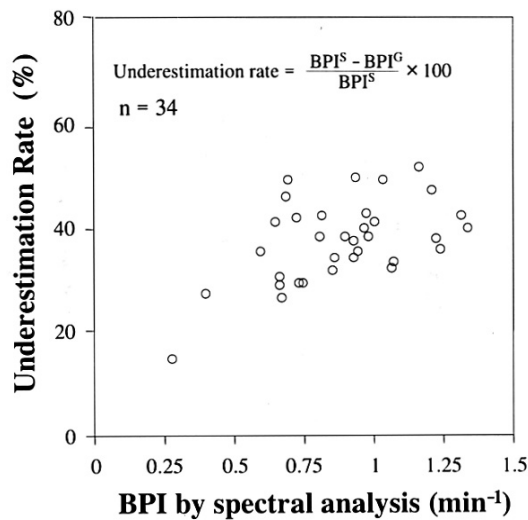


Fig. 3 Underestimation rate in BPI^{G} compared with BPI^{S} . The degree of the underestimation rate tended to increase as the BPI^{S} values increased.

and CBF^{PET} values are significantly correlated ($r = 0.881$), with a regression equation of $y = 0.020x - 0.023$. Although the BPI^{G} and CBF^{PET} values also significantly correlated ($r = 0.832$), with a regression equation of $y = 0.011x + 0.066$, the correlation coefficient for BPI^{G} was lower than for BPI^{S} . The absolute value of the intercept for the BPI^{S} line was smaller than that for BPI^{G} .

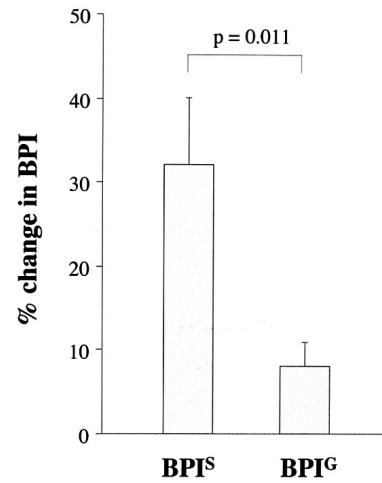


Fig. 4 Comparison of the degree of increase in BPI (% change in BPI). The % change in BPI^{S} was significantly larger than that in BPI^{G} (Wilcoxon signed rank test).

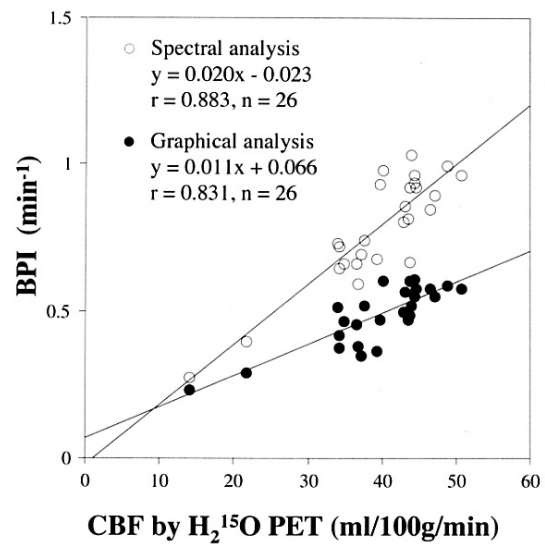


Fig. 5 Relationship between the BPI values obtained by means of SA (BPI^{S} , open circles) or GA (BPI^{G} , closed circle) using ^{99m}Tc -HMPAO (y) and the cerebral blood flow values measured by using H_2O PET (CBF^{PET}) (x). The correlation between the BPI and CBF^{PET} values was statistically significant ($p < 0.01$) in both SA and GA.

DISCUSSION

SA has previously been used for the analysis of dynamic PET scans in humans. This imaging technique provides data consisting of the time courses of the activities in tissue regions of interest and in arterial blood following the administration of a radiolabeled tracer.⁷ This technique results in a simple spectrum of kinetic components that relate the tissue's response to the blood activity curve. This technique facilitates the interpretation of dynamic

PET data and simplifies comparisons between regions and between subjects.

Murase et al. applied this SA method to dynamic SPECT data using ^{123}I -IMP and compared its usefulness with that of compartment analysis.⁸ Furthermore, Murase et al.⁹ showed that BPI obtained by SA using $^{99\text{m}}\text{Tc}$ -HMPAO was significantly associated with the CBF that was obtained by using ^{123}I -IMP and the modified early (ME) method¹⁴ with continuous arterial blood sampling. They thus demonstrated that the SA method is a simple, non-invasive and useful tool for the quantitative evaluation of CBF. However, only a few studies have compared BPI by SA using technetium-99m labeled compounds with the absolute CBF measured by H_2^{15}O PET, which most precisely reflects the real CBF.

The quantification of CBF using BPI is effective when BPI accurately reflects the CBF. Murase et al. showed two crucial advantages in estimating BPI using SA.⁹ First, BPI by SA is hardly affected by the conversion of a lipophilic, diffusible tracer to a hydrophilic, non-diffusible tracer in the arterial blood of the brain.⁹ This influence of $^{99\text{m}}\text{Tc}$ -HMPAO in humans results in a 1.0% difference in BPI, at most.⁹ Thus, this effect might be negligible for technetium-99m labeled compounds when BPI is measured using SA. Second, with SA, BPI is hardly affected by the first-pass extraction fraction.

In this study, the BPI^{G} values were underestimated compared with the BPI^{S} values (Fig. 3). The degree of underestimation tended to increase as the BPI^{S} values increased. These results agree with those of previous report.⁹ This underestimation is probably a result of the fact that the BPI^{G} values are affected by the first-pass extraction fraction of the tracer.^{8,9} Matsuda et al. indicated that BPI^{G} represents the unidirectional influx rate from the blood to the brain and is proportional to the product of the CBF and the first-pass extraction fraction of the tracer.^{4,5} Thus, BPI^{G} does not truly reflect CBF, especially when the first-pass extraction fraction of the tracer used is low. The first-pass extraction fraction decreases with an increase in CBF,¹⁵ implying that the deviation between CBF and BPI^{G} increases with an increase in CBF. This could be problematic, especially when measuring increased CBF during activation studies, such as carbon dioxide inhalation or ACZ injection,¹⁶ or when detecting hyperperfused areas, such as in cases of infarction^{17,18} or epilepsy.^{19,20}

We also studied the changes in BPI after ACZ injection in four healthy volunteers (Fig. 4). Our study showed that the percent increase in BPI^{G} ($8.1 \pm 2.8\%$) was significantly lower than that in BPI^{S} ($32.1 \pm 8.0\%$). The value of percent increase in BPI^{S} was almost equal to the degree of increase in CBF measured using H_2^{15}O PET, according to previous reports.^{9,21,22} This fact suggest that BPI^{S} was less affected by the first-pass extraction fraction of the tracer even when the first-pass extraction fraction is lower and changes in proportion to the CBF. Thus, BPI by SA might

be more linearly correlated with the absolute CBF, even when the CBF is elevated as a result of pharmacological intervention or for some clinical situations, such as an early postischemic hyperperfused state or epileptic state.

In our study, we measured both BPI and CBF by using H_2^{15}O PET in 13 patients. The BPI^{S} and CBF^{PET} values showed a significant correlation. Although the BPI^{G} and CBF^{PET} values were also significantly correlated, the correlation coefficient for BPI^{G} was lower than that for BPI^{S} . Furthermore, the absolute value of the intercept of the BPI^{S} line was smaller than that of BPI^{G} . These findings largely correspond with those of a previous report using ^{123}I -IMP.⁸ These results suggest that SA should provide a more reliable BPI than GA in proportion to the absolute CBF. Thus, BPI by SA should be more closely correlated with the absolute CBF when measuring elevated CBF levels.

CONCLUSION

We have demonstrated a simple, non-invasive and useful method for the quantitative evaluation of CBF. We have showed that BPI by SA is linearly correlated with the absolute CBF measured by using H_2^{15}O PET. Our results suggest that this novel SA method will provide a more reliable measurement of BPI for the quantification of CBF using $^{99\text{m}}\text{Tc}$ -HMPAO than the conventional procedure using GA. This feature is of particular clinical significance, especially when performing activation studies using pharmacological intervention, such as acetazolamide infusion, or for clinically important states.

APPENDIX

Blood flow [F] can be determined from the value of tissue impulse response function [$\text{IRF}(t)$] at time zero in the following fashion. The concentration of a tracer within a tissue at time t [$C_{\text{tissue}}(t)$] is determined from Fick's principle as

$$C_{\text{tissue}}(t) = \int_{-\infty}^t F [C_{\text{in}}(u) - C_{\text{out}}(u)] du, \quad \text{Eq. A1}$$

assuming that the system describing the flow of tracer into and through the tissue is linear and stationary.²³ In Eq. A1, $C_{\text{in}}(t)$ and $C_{\text{out}}(t)$ represent the concentration of the tracer within the blood flowing into and out of the tissue, respectively.

If the input into the system is instantaneous and occurs at time zero, then $C_{\text{tissue}}(t)$ can be replaced by $S \cdot \text{IRF}(t)$ and $C_{\text{in}}(t)$ by Dirac's delta function multiplied by $S[S \cdot \delta(t)]$, with S being the scale factor given by

$$S = \int_{-\infty}^{\infty} C_{\text{in}}(t) dt. \quad \text{Eq. A2}$$

Thus, is given by

$$\text{ITF}(t) = \int_{-\infty}^t F \left[\delta(u) - \frac{C_{\text{out}}(u)}{S} \right] du, \quad \text{Eq. A3}$$

yielding

$$\text{INF}(0) = F. \quad \text{Eq. A4}$$

This indicates that the BPI^S given by Eq. 3 is proportional to CBF.

ACKNOWLEDGMENTS

The authors would like to thank the staff of the Department of Nuclear Medicine and the Cyclotron staff of Osaka University Hospital for their technical support in performing the studies and Ms. M. Sudo and K. Tsunoda for their administrative assistance.

Masashi Takasawa is a doctoral student supported by the Japan Society for the Promotion of Science.

REFERENCES

1. Hellman RS, Tikofsky RS. An overview of the contributions of regional cerebral blood flow studies in cerebrovascular disease: is there a role for single photon emission computed tomography? *Semin Nucl Med* 1990; 20: 303–324.
2. Nakano S, Kinoshita K, Jinnouchi S, Hoshi H, Watanabe K. Critical cerebral blood flow thresholds studied by SPECT using xenon-133 and iodine-123 iodoamphetamine. *J Nucl Med* 1989; 30: 337–342.
3. Takasawa M, Watanabe M, Yamamoto S, Hoshi T, Sasaki T, Hashikawa K, et al. Prognostic value of subacute crossed cerebellar diaschisis: single-photon emission CT study in patients with middle cerebral artery territory infarct. *AJNR Am J Neuroradiol* 2002; 23: 189–193.
4. Matsuda H, Tsuji S, Shuke N, Sumiya H, Tonami N, Hisada K. A quantitative approach to technetium-99m hexamethylpropylene amine oxime. *Eur J Nucl Med* 1992; 19: 195–200.
5. Matsuda H, Yagishita A, Tsuji S, Hisada K. A quantitative approach to technetium-99m ethyl cysteinate dimer: a comparison with technetium-99m hexamethylpropylene amine oxime. *Eur J Nucl Med* 1995; 22: 633–637.
6. Lassen NA, Anderson AR, Friberg L, Paulson OB. The retention of [^{99m}Tc]-L,D-HMPAO in the human brain after intracarotid bolus injection: a kinetic analysis. *J Cereb Blood Flow Metab* 1988; 8 (Suppl 1): S44–S51.
7. Cunningham VJ, Jones T. Spectral analysis of dynamic PET studies. *J Cereb Blood Flow Metab* 1993; 13: 15–23.
8. Murase K, Tanada S, Inoue T, Ikezoe J. Spectral analysis applied to dynamic single photon emission computed tomography studies with *N*-isopropyl-*p*-(¹²³I)iodoamphetamine. *Ann Nucl Med* 1998; 12: 109–114.
9. Murase K, Inoue T, Fujioka H, Ishimaru Y, Akamune K, Yoshimoto Y, et al. An alternative approach to estimation of the brain perfusion index for measurement of cerebral blood flow using technetium-99m compounds. *Eur J Nucl Med* 1999; 26: 1333–1339.
10. Takasawa M, Murase K, Oku N, Yoshikawa T, Osaki Y, Imaizumi M, et al. Assessment of acetazolamide reactivity in cerebral blood flow using spectral analysis and technetium-99m hexamethylpropylene amine oxime. *J Cereb Blood Flow Metab* 2002; 22: 1004–1009.
11. Takasawa M, Murase K, Oku N, Kawamata M, Imaizumi M, Yoshikawa T, et al. Automatic determination of brain perfusion index for measurement of cerebral blood flow using spectral analysis and ^{99m}Tc-HMPAO. *Eur J Nucl Med* 2002; 29: 1443–1446.
12. Haug SC. Quantitative measurement of local cerebral blood flow in humans by positron emission tomography and ¹⁵O-water. *J Cereb Blood Flow Metab* 1983; 3: 141–153.
13. Llacer J, Veklerov E, Baxter LR, Grafton ST, Griffeth LK, Hawkins RA, et al. Results of a clinical receiver operating characteristic study comparing filtered backprojection and maximum likelihood estimator images in FDG PET studies. *J Nucl Med* 1993; 34: 1198–1203.
14. Inoue T, Fujioka H, Akamune A, Tanada S, Hamamoto K. A time-saving approach for quantifying regional cerebral blood flow and application to split-dose method with ¹²³I-IMP SPECT using a single-head rotating gamma-camera [in Japanese]. *KAKU IGAKU (Jpn J Nucl Med)* 1995; 32: 1217–1226.
15. Murase K, Tanada S, Fujita H, Sakaki S, Hamamoto K. Kinetic behavior of technetium-99m-HMPAO in the human brain and quantification of cerebral blood flow using dynamic SPECT. *J Nucl Med* 1992; 33: 135–143.
16. Buell U, Schicha H. Nuclear medicine to image applied pathophysiology: evaluation of reserves by emission computerized tomography. *Eur J Nucl Med* 1990; 16: 129–135.
17. Marchal G, Young AR, Baron JC. Early postischemic hyperperfusion: pathophysiologic insights from positron emission tomography. *J Cereb Blood Flow Metab* 1999; 19: 467–482.
18. Takasawa M, Watanabe M, Yuasa Y, Iiji O, Hashikawa K, Matsumoto M, et al. Transient patchy boundary zone hyperemia following TIA episode with deep hemispheric ischemia: serial HMPAO SPECT study. *J Neurol* 2000; 247: 804–806.
19. Lassen NA, Spering B. ^{99m}Tc-bicisate reliably images CBF in chronic brain diseases but fails to show reflow hyperemia in subacute stroke: report of a multicenter trial of 105 cases comparing ¹³³Xe and ^{99m}Tc-bicisate (ECD, neorolite) measured by SPECT on same day. *J Cereb Blood Flow Metab* 1994; 14: S44–S48.
20. Camargo EE. Brain SPECT in neurology and psychiatry. *J Nucl Med* 2001; 42: 611–623.
21. Hayashida K, Tanaka K, Hirose Y, Kume N, Iwama T, Miyake Y, et al. Vasoreactive effect of acetazolamide as a function of time with sequential PET O15-water measurement. *Nucl Med Commun* 1996; 17: 1047–1051.
22. Kuwabara Y, Ichiya Y, Sasaki M, Yoshida T, Fukumura T, Masuda K, et al. PET evaluation of cerebral hemodynamics in occlusive cerebrovascular disease pre- and postsurgery. *J Nucl Med* 1998; 39: 760–765.
23. Gobbel GT, Fike JR. A deconvolution method for evaluating indicator-dilution curves. *Phys Med Biol* 1994; 39: 1833–1854.